TISSUE ENGINEERING: Part A
Volume 20, Numbers 13 and 14, 2014

DOI: 10.1089/ten.tea.2013.0496

Dynamic Vibration Cooperates with Connective Tissue Growth Factor to Modulate Stem Cell Behaviors

Zhixiang Tong, PhD,[1,*] Aidan B. Zerdoum, BS,[2] Randall L. Duncan, PhD,[2–4] and Xinqiao Jia, PhD[1,2]

Vocal fold disorders affect 3–9% of the U.S. population. Tissue engineering offers an alternative strategy for vocal fold repair. Successful engineering of vocal fold tissues requires a strategic combination of therapeutic cells, biomimetic scaffolds, and physiologically relevant mechanical and biochemical factors. Specifically, we aim to create a vocal fold-like microenvironment to coax stem cells to adopt the phenotype of vocal fold fibroblasts (VFFs). Herein, high frequency vibratory stimulations and soluble connective tissue growth factor (CTGF) were sequentially introduced to mesenchymal stem cells (MSCs) cultured on a poly(ε-caprolactone) (PCL)-derived microfibrous scaffold for a total of 6 days. The initial 3-day vibratory culture resulted in an increased production of hyaluronic acids (HA), tenascin-C (TNC), decorin (DCN), and matrix metalloproteinase-1 (MMP1). The subsequent 3-day CTGF treatment further enhanced the cellular production of TNC and DCN, whereas CTGF treatment alone without the vibratory preconditioning significantly promoted the synthesis of collagen I (Col 1) and sulfated glycosaminoglycans (sGAGs). The highest level of MMP1, TNC, Col III, and DCN production was found for cells being exposed to the combined vibration and CTGF treatment. Noteworthy, the vibration and CTGF elicited a differential stimulatory effect on elastin (*ELN*), HA synthase 1 (*HAS1*), and fibroblast-specific protein-1 (*FSP-1*). The mitogenic activity of CTGF was only elicited in naïve cells without the vibratory preconditioning. The combined treatment had profound, but opposite effects on mitogen-activated protein kinase (MAPK) pathways, Erk1/2 and p38, and the Erk1/2 pathway was critical for the observed mechano-biochemical responses. Collectively, vibratory stresses and CTGF signals cooperatively coaxed MSCs toward a VFF-like phenotype and accelerated the synthesis and remodeling of vocal fold matrices.

Introduction

Vocal folds are soft connective tissues that effectively convert aerodynamic energy to audible pulses for sound production.[1,2] Vocal folds are composed of a stratified squamous epithelium, a matrix-rich lamina propria (LP), and the vocalis muscle. Adult human vocal fold LP is a highly organized and complex structure, consisting of a superficial layer (SLP) lacking mature collagen and elastin fibers, an intermediate layer (ILP) rich in elastin and hyaluronic acid (HA), and a deep layer (DLP) with abundant collagen fibers and other interstitially dispersed proteoglycans.[3] While the SLP is essential for the free flow of the mucosal wave, the vocal ligament, ILP, and DLP combined, provides sufficient strength to the tissue during phonation. Adult vocal folds experience a broad frequency range (100–300 Hz) and sustain strains up to 30% during normal phonation.[1,2]

Human vocal folds are frequently exposed to numerous insults, such as voice abuse, infections, or chemical irritants. Once these physiological provocations exceed the tissue's healing capacity, vocal scarring or dysphonia occurs. Vocal fold scarring is associated with altered matrix composition and tissue mechanics, therefore compromising the SLP's ability to propagate the mucosal wave during phonation.[2–4] Stem cell-based tissue engineering strategy has emerged as a promising alternative approach for vocal fold restoration.[5] Mesenchymal stem cells (MSCs) have been widely employed as the therapeutic cells for a variety of regenerative medicine applications.[6,7] MSCs are a suitable alternative to primary vocal fold fibroblasts (VFFs) for vocal fold tissue engineering, considering their similar phenotype, multipotency, and immunoregulatory functions.[6,8] Mounting evidence confirms the regulatory role of the tissue-specific microenvironment in controlling the behaviors of MSCs.[9–11]

[1]Department of Materials Science and Engineering, Delaware Biotechnology Institute, University of Delaware, Newark, Delaware.
[2]Biomedical Engineering Program, University of Delaware, Newark, Delaware.
Departments of [3]Biological Sciences and [4]Mechanical Engineering, University of Delaware, Newark, Delaware.
Current affiliation: Division of Biomedical Engineering, Department of Medicine, Center for Regenerative Therapeutics, Brigham and Women's Hospital, Harvard Medical School, Cambridge, Massachusetts.

We are interested in developing tissue engineering methodologies for vocal fold regeneration. The primary goal of this investigation is to create a vocal fold-like stem cell niche to coax MSCs to adopt the behaviors of VFFs.

Successful engineering of vocal fold tissue requires a fundamental understanding of vocal fold development. Being the major type of cells in vocal fold, VFFs are responsible for the synthesis and the maintenance of LP extracellular matrix (ECM). Newborn vocal fold LP is structurally and compositionally homogeneous, consisting mainly of ground substances, lacking the layered matrix organization seen in adult vocal folds. It has been suggested that phonation-related mechanical stresses and local hormonal signaling are the key contributing factors for vocal fold maturation.[12,13] It is generally accepted that the tension generated during phonation after birth activates the resident fibroblasts in macula flava, resulting in an accelerated matrix deposition during vocal fold development.[14] We have previously demonstrated that high frequency vibrations can alter the gene expression by MSCs cultivated on an electrospun fibrous scaffold.[6,15] On the other hand, vocal fold development and maturation are influenced by various growth factors; higher levels of hormone receptors and/or serum hormones in male vocal folds are, to some extent, correlated with the elevated level of HA found in male vocal folds.[16] Our previous work confirmed the regulatory role of connective tissue growth factor (CTGF) on MSC differentiation toward VFF-like cells.[15] CTGF is a multi-domain protein that binds various integrin receptors or heparin sulfate proteoglycans to orchestrate diverse cellular events in embryonic development, angiogenesis, mitogenesis, tissue morphogenesis, and wound healing and fibrosis.[15,17,18]

We hypothesize that physiologically relevant vibratory forces and soluble biochemical cues will cooperatively drive MSCs toward the VFF phenotype.[6,18–21] In the present study, we explore the effects of combined vibratory stimulations and soluble CTGF on MSCs in terms of their proliferation, gene expression, and protein synthesis. In our study, MSCs were subjected to 3-day vibratory culture without CTGF, followed by 3-day static culture in the presence of CTGF. We also examined the role of mitogen-activated protein kinase (MAPK) pathways in mediating cellular responses to aforementioned stimulations. Overall, the combined mechanical and biochemical cues cooperatively enhanced MSC's ability to synthesize essential vocal fold ECM molecules, to remodel their matrices, and to adopt the fibroblastic phenotype.

Materials and Methods

Scaffold fabrication and characterization

Fibrous PCL scaffolds were fabricated by electrospinning as previously described with minor changes.[6] Briefly, a chloroform solution of PCL (M_n ~80 kDa, 15 wt%) (Sigma Aldrich, St. Louis, MO) was spun from a 10 mL syringe locked to a programmable syringe pump (New Era Pump Systems, Farmingdale, NY). The flow rate, spinning voltage, and needle-to-collector distance was set at 1.5 mL/h, 15 kV and 18 cm, respectively. The collected meshes (thickness: 250–300 μm) were cut into four-arm-shaped disks (dry weight: 12.6 ± 0.4 mg, diameter: 12 mm) for facial insertion into the vibration chamber.[6] To improve the hydrophilicity of the PCL scaffolds, individual disks were immersed in 70% ethanol for 12 h, hydrolyzed with 0.5 N NaOH for 1 h at 37°C, and further neutralized with 0.01 N HCl for 5 min.[22] The morphology of the as-spun and surface-modified PCL fibers was characterized using a field-emission scanning electron microscope (FE-SEM, JSM-7400F; JEOL-USA, Peabody, MA).

Vibratory culture and CTGF treatment

A custom-designed, vibratory bioreactor was employed to simulate the mechanical environment of vibrating vocal folds. The readers are referred to our previous publication for detailed description on the vocal fold bioreactor.[6] Briefly, the bioreactor is composed of two metal bars (1, Fig. 1A), each housing four parallel vibration modules (2, Fig. 1A). The individual module (a and b, Fig. 1A) containing a sandwiched silicone elastomer (b(iii), Fig. 1A) is directly mounted on top of a speaker (a(i) and 3, Fig. 1A) that is controlled by a speaker selector (4, Fig. 1A, Radio-Shack, Fort Worth, TX). The vibration units and speaker selector are enclosed in an anti-humidity acrylic chamber (5, Fig. 1A). The assembly containing 1–5 (Fig. 1A) is housed in the cell culture incubator, while the power amplifier and the function generator are placed outside. Separately, the surface-modified PCL mats (b(ii), Fig. 1A) were sterilized by germicidal UV light (6 min each side), rinsed with copious DPBS (Invitrogen, Carlsbad, CA) before being placed in the vibration module for cell seeding.[6] Human bone marrow-derived MSCs (passage 3–4, Lonza, Walkersville, MD) were grown in MSC maintenance medium (Lonza) in a humidified incubator at 37°C with 5% CO_2. At 80–90% confluence, cells were trypsinized, centrifuged, and re-suspended in the maintenance media. Forty microliters of cell suspension (~4×10^6 cells/mL) was evenly seeded on the scaffold and cells were allowed to adhere for 1–1.5 h before additional MSC maintenance media (1.5 mL) were added. Three days post seeding (designated as day 0 in the context of vibratory stimulation and CTGF treatment, Fig. 1B), sinusoidal vibrations were introduced in a 1h-on-1h-off pattern for 12 h daily for 3 days.[6] The vibration frequency and the normal displacement at the center of the scaffold were maintained at 200 Hz and 40 μm, respectively. After 3 days of dynamic culture, cell culture media was replaced with that supplemented with 100 ng/mL CTGF (Biovendor, Asheville, NC) and 50 μg/mL ascorbic acids (Sigma),[15] and MSCs were cultured statically from day 3 to 6 (Fig. 1B). The media was refreshed every other day during the dynamic culture, but was changed daily during the CTGF treatment, considering the short half-life of CTGF.[23] To confirm the involvement of the Erk1/2 pathway, an Erk1/2 inhibitor, U0126 (10 μM; Cell Signaling, Danvers, MA), was added to the media surrounding the cellular constructs on day 3. Two hours later, the constructs were rinsed with DPBS and were subsequently cultured in the CTGF-containing media for 22 h. On days 4 and 5, the 2-h U0126 inhibition protocol was repeated. On day 0, 3, and 6, cellular constructs, with or without the U0126 inhibition, were harvested and snap frozen for gene and protein analyses. In addition, the cell culture supernatants pooled from day 3 to 6 were stored at −20°C for future enzyme-linked immunosorbent assays (ELISA). Various control groups, with or

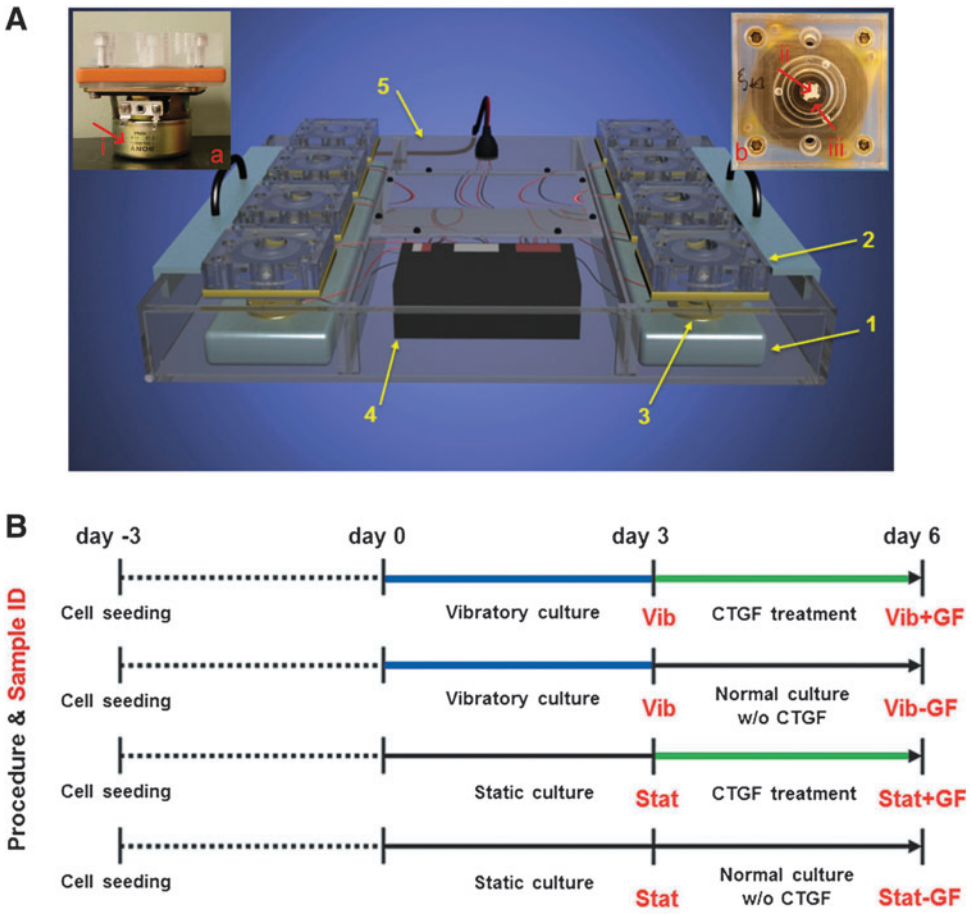

FIG. 1. Bioreactor design and cell culture protocol. **(A)** Schematic illustration of the bioreactor assembly. (1): stationary metal bar; (2): vibration module; (3): speaker; (4): speaker selector; (5): acrylic anti-humidity chamber. Inserts: a side (a) and a top (b) view of an individual vibration module, (i): speaker; (ii): poly(ε-caprolactone) (PCL) mat (white); (iii): silicone elastomer (transparent) that serves the bottom of the chamber. **(B)** Flowchart illustrating the sequential introduction of mechanical and biochemical stimulations. Three days post seeding (day 0), MSCs were subjected to a 3-day vibratory stimulation (timeline highlighted in blue) without connective tissue growth factor (CTGF), followed by a 3-day static culture in the presence of CTGF (timeline highlighted in green). Vib: vibratory culture; Stat: static culture; Vib + GF: vibratory culture followed by CTGF treatment; Vib–GF: vibratory culture followed by standard culture without CTGF; Stat + GF: static culture followed by CTGF treatment; Stat–GF: static culture followed by standard culture without CTGF. Color images available online at www.liebertpub.com/tea

without vibratory culture or CTGF treatment (Fig. 1B), were included for comparison purposes. Samples collected at day 3 were designated as Vib and Stat and those collected at day 6 were referred to as Vib + GF, Vib − GF, Stat + GF, and Stat − GF, with Vib and Stat representing vibratory and static culture, respectively, and + GF and − GF indicating the presence or the absence of CTGF, respectively.

DNA and sulfated glycosaminoglycan quantification

DNA content per scaffold was quantified by Picogreen DNA assay (Invitrogen). Specifically, the collected constructs were enzymatically digested in a sodium phosphate buffer (Sigma Aldrich) containing 10 mM Na_2EDTA, 100 mM Na_2PO4, 10 mM L-cysteine, and 0.2 mg/mL papain at pH 6.5 at 63°C for 16–18 h.[24] The digestion was subsequently centrifuged at 12,000 *g* for 5 min, and the supernatant was aliquoted (10 µL) immediately for DNA assay following the manufacturer's instruction. Separate aliquots of the papain digestion were used in the dimethylmethylene blue (DMB) assay for sulfated glycosaminoglycan (sGAG) quantification. Briefly, 5 mL of a 3.2 mg/mL DMB stock solution in 100% ethanol was added to 900 mL of NaCl (40 mM)-glycine (40 mM) solution and DI H_2O to obtain a DMB working solution (1 L, 16 µg/mL, pH = 3.0). The papain-digested samples (40 µL) and the sGAG standards (0–20 µg/mL, Biocolor, United Kingdom) were thoroughly mixed with 250 µL DMB working solution in a 96-well plate (Corning, NY). The absorbance of the mixture was immediately measured at 530 nm (abs.) using a PerkinElmer microplate reader.

Real-time polymerase chain reaction

RNA was extracted and purified from the snap-frozen constructs as reported previously.[6] The RNA samples (0.5 µg each) were reverse transcribed to cDNA utilizing a QuantiTect reverse transcription kit (Qiagen, Valencia, CA). Quantitative polymerase chain reaction (qPCR) was performed on an ABI 7300 real-time sequence detection

system. A 20 μL reaction solution containing 400 nM primer mix, 4 ng cDNA and 10 μL Power SYBR green master mix (2×; Invitrogen) was prepared for each reaction. The primer sequence, the amplification efficiency and the product size have been previously documented.[6] All the primers were manufactured by Integrated DNA Technologies (Coralville, IA). The qPCR data were analyzed using qbasePLUS software (V2.5; Biogazelle, Ghent, Belgium).[6]

Western analysis

Cellular constructs were lysed using a standard ice-cold radio-immunoprecipitation assay buffer, supplemented with phosphatase inhibitors (1%), protease inhibitor cocktail (1%), and 5 mM EDTA (all from Thermo Scientific, Waltham, MA). The lysis mixture was snap frozen on an isopropanol/dry ice-cold bath for 3 min, sonicated, and thawed in an ultrasonic bath (Cole Parmer, Vernon Hills, IL) for 3–5 min at room temperature. This freeze-thaw cycle was repeated four times before the constructs were heated at 95°C for 5 min to ensure complete protein solubilization. The protein lysate was subsequently centrifuged at 13,000 g for 15 min at 4°C to remove any insoluble debris. The protein concentration in the filtrates was quantified using a Micro BCA Protein Assay Kit (Thermo Scientific) following the manufacturer's protocol. The protein extracts (5 μg each), premixed with 25% Laemmli sample buffer (4×) and 5% 2-mercaptoethanol (both from Bio-Rad, Hercules, CA), were boiled at 99°C for 8 min before electrophoresis. Immediately after boiling, the protein mixture was separated on a 10% Mini-PROTEAN TGX™ Precast Gel (Bio-Rad) for 90 min at 100 V. Prestained protein ladders (10-250 kDa; Thermo Scientific) were included as the molecular weight standards. The resolved proteins were transferred to a nitrocellulose membrane (Bio-Rad) at 4°C for 2 h at 400 mA. After being blocked with 5% BSA in tris-buffered saline containing 0.2% Tween-20 (TBST) at 4°C overnight, the membrane was incubated for 2–3 h at room temperature with monoclonal primary antibodies against human type I and type III collagen and GAPDH (Abcam, Cambridge, MA), total Erk1/2, total p38, phospho-Erk1/2 and phospho-p38 (Cell Signaling), and BA4 mouse anti-elastin (Sigma). The primary antibodies were diluted from 1:300–1:2000 in TBST with 2% BSA. The incubation was conducted in a mini-strip blotting box (Fisher Scientific) with gentle shaking. After three washes with TBST, the membrane was incubated with goat anti-rabbit or mouse Poly-HRP secondary IgG (Thermo Scientific) at a 1:4000–1:20,000 dilution for 45 min, followed by four vigorous washes (10 min each) with TBST. Finally, the immunoblots were treated with Amersham ECL Prime western blotting reagent (GE Healthcare Bioscience, Piscataway, NJ) and exposed to HyBlot CL autoradiography X-ray film (Denville Scientific, Metuchen, NJ) for 10 s – 5 min. Films were developed using a Kodak film developer (Rochester, NY). The resulting images were scanned and processed for densitometry analyses using Image J software (http://rsb.info.nih.gov/ij/).

ELISA analysis

ELISA were carried out to quantify cellular production of HA, tenascin-C (TNC), matrix metalloproteinase-1 (MMP1), and decorin (DCN).[6] The collected media samples were diluted and assayed for HA using an HA competitive ELISA kit (Echelon Biosciences, Salt Lake City, UT). The production of TNC (high molecular weight variant) was assayed using a solid phase sandwich ELISA kit (Immuno-Biological Laboratories, Gunma, Japan). Cellular production of MMP1 and DCN was quantified using their corresponding DuoSet ELISA Development kits from R&D systems (Minneapolis, MN).

Statistical analysis

All quantitative results were represented as the mean ± standard error of the mean (SEM) with $n \geq 3$. Student's two-tailed t test was used to determine the significant differences between Vib and Stat samples at day 3, with $p < 0.05$ being considered to be statistically different. Two-way ANOVA analysis, followed by Tukey–Kramer *post-hoc* test, was performed for the multiple comparisons among different groups at day 6, with $p < 0.05$ being considered as statistically significantly different.

Results

In this study, we investigated the effects of mechanical and biochemical cues, introduced sequentially, on MSCs cultured on fibrous PCL scaffolds. The as-spun scaffolds were subjected to alkaline hydrolysis prior to cell culture.[22] The surface modification did not alter the fiber diameter, morphology, or surface topography (Supplementary Fig. S1; Supplementary Data are available online at www.liebertpub.com/tea). In both cases, the average fiber diameter was estimated to be ~5 μm and individual fibers were randomly oriented. The nanoscale holes seen on fiber surface is a result of atmospheric water droplet formed during electrospinning.[25] The surface modification rendered the PCL scaffold more hydrophilic, as evidenced by the rapid spreading and penetration of the cell culture media into the scaffold. MSCs readily attached to the scaffolds and were evenly distributed on the scaffold 3 days after seeding (data not shown), in agreement with our previous observations.[6] Cells were first subjected to vibration stimulations for 3 days in MSC maintenance media. A vibration frequency of 200 Hz was chosen to represent the average fundamental speaking frequency of male and female adults, and a mid-membrane normal displacement of 40 μm was selected to maximize the device performance and to minimize interference from the harmonic signals and liquid agitation.[6] Cells were subsequently cultured statically for 3 days in the presence of CTGF (Fig. 1B). Cellular responses to mechanical stimulations and biochemical cues were collectively evaluated by *q*PCR, western blotting, and ELISA. Mechanistic studies were conducted to ascertain the involvement of Erk1/2 in cell signaling.

Effects of mechanical and biochemical stimulations on MSC functions

Picogreen DNA analysis (Fig. 2) revealed that the DNA content per scaffold at day 3 was slightly, but not significantly, elevated compared to day 0, irrespective of the culture conditions (Vib vs. Stat). On the other hand, constructs subjected to 3-day vibratory culture exhibited a significantly higher DNA content on day 6 relative to day 0, regardless of the media composition (Vib – GF and Vib + GF). Cells cultured statically without CTGF for 6 days (Stat – GF) did not proliferate

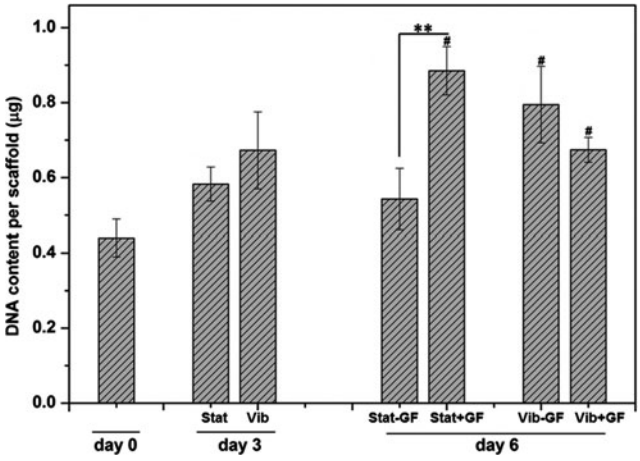

FIG. 2. Cell proliferation, as quantified by Picogreen DNA assay, as a function of culture time and conditions. Average scaffold weight (dry): ~12.6 mg. #Significantly higher than the day 0 level ($p < 0.05$). **Significantly different between the indicated groups ($p < 0.05$).

significantly relative to day 0 ($p > 0.1$). MSCs in the Stat + GF group proliferated more than those in the Stat − GF group at day 6 ($p < 0.05$). Within 6 days, the cell number in the Stat + GF group had more than doubled ($p < 0.05$). Thus, the mitogenic effect of CTGF was only observed when cells were cultured statically, suggesting that the dynamic preconditioning may have suppressed the mitogenic effects of CTGF on MSCs.

Next, the modulatory effects of mechanical and biochemical stimulations on MSC gene expression were analyzed by qPCR. To simplify our discussion, genes were grouped into four categories: (1) those encoding ECM proteins found in vocal fold LP, (2) those encoding putative fibroblastic hallmarks and ECM enzymes, and (3) those encoding typical MSCs differentiation markers. In general, genes in each group displayed similar expression patterns throughout the 6 days of individual or combined stimulations. Compared with the static controls at day 3, the relative expression of *HAS1* (Fig. 3A) by cells in the Vib groups was significantly elevated (from 0.86 ± 0.05 for Stat to 1.58 ± 0.28 for Vib, $p < 0.05$). While *HAS1* expression by Stat + GF at day 6 was significantly higher than that expressed by the Stat group at day 3 (~1.57-fold, $p < 0.05$), additional 3 days of static culture without CTGF did not alter the *HAS1* expression (Stat − GF vs. Stat). Interestingly, CTGF-induced overexpression of *HAS1* was not found in groups that had been subjected to prior vibratory stimulations. In other words, *HAS1* expression by Vib + GF and Vib − GF groups was not statistically different. However, vibration-induced upregulation of *HAS1* was maintained during the following 3 days of static culture, regardless of the media composition. Vibratory culture also led to a significant upregulation of *DCN* expression ($p < 0.001$, Fig. 3B), as evidenced by a 0.81 ± 0.03 and 1.21 ± 0.04-fold change relative to the day 0 level for Stat and Vib cultures, respectively. Subsequent 3-day CTGF treatment resulted in further upregulation of *DCN* expression in the Vib + GF (2.00 ± 0.23 Fold) group and in the Vib − GF (1.50 ± 0.13 Fold) group. Overall, *DCN* expression at day 6 by the Vib + GF group was significantly higher than by the Stat + GF group (~1.89-fold, $p < 0.01$).

Similar vibration-induced responses were observed for other important ECM proteins found in vocal folds. For instance, the vibratory preconditioning increased the *ELN* expression (Fig. 3C) by approximately two-folds at day 3 (Stat vs. Vib, $p < 0.05$). *ELN* expression was significantly ($p < 0.05$) elevated at day 6 for Vib − GF and Vib + GF,

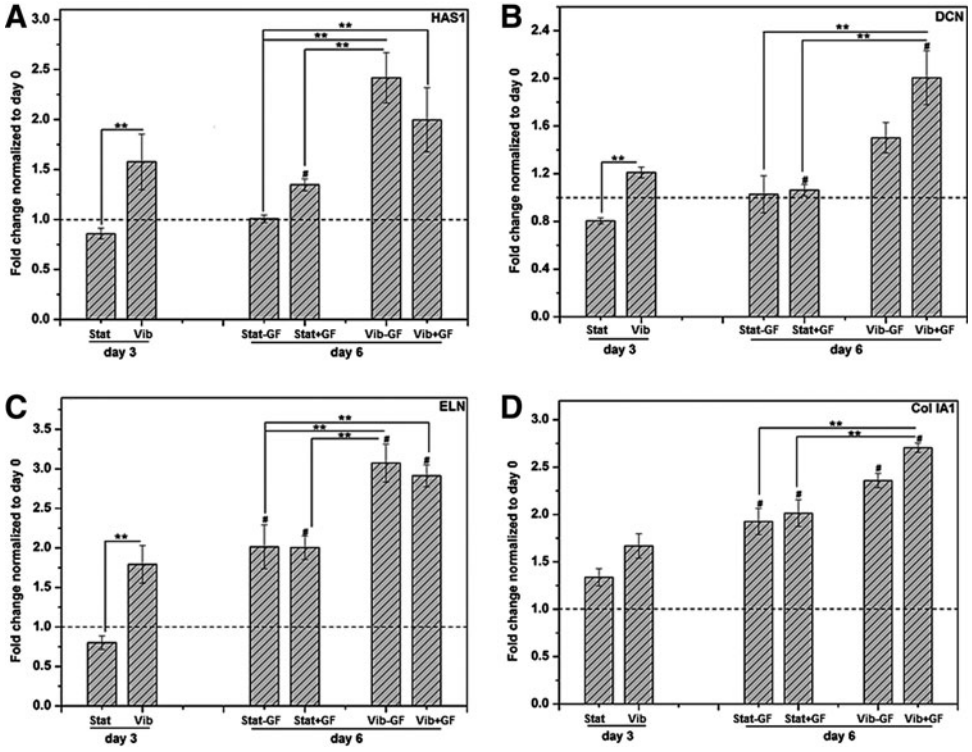

FIG. 3. Effects of the culture time and conditions on the expression of genes encoding important extracellular matrix (ECM) proteins (**A**: hyaluronic synthase (*HAS1*), **B**: decorin (*DCN*), **C**: elastin (*ELN*), **D**: collagen 1A1 (*Col 1A1*)). The relative expression (fold change) was normalized to the level at day 0 (dashed baseline). #Significantly different compared with the corresponding static or dynamic culture at day 3 ($p < 0.05$); **significantly different between the indicated groups ($p < 0.05$).

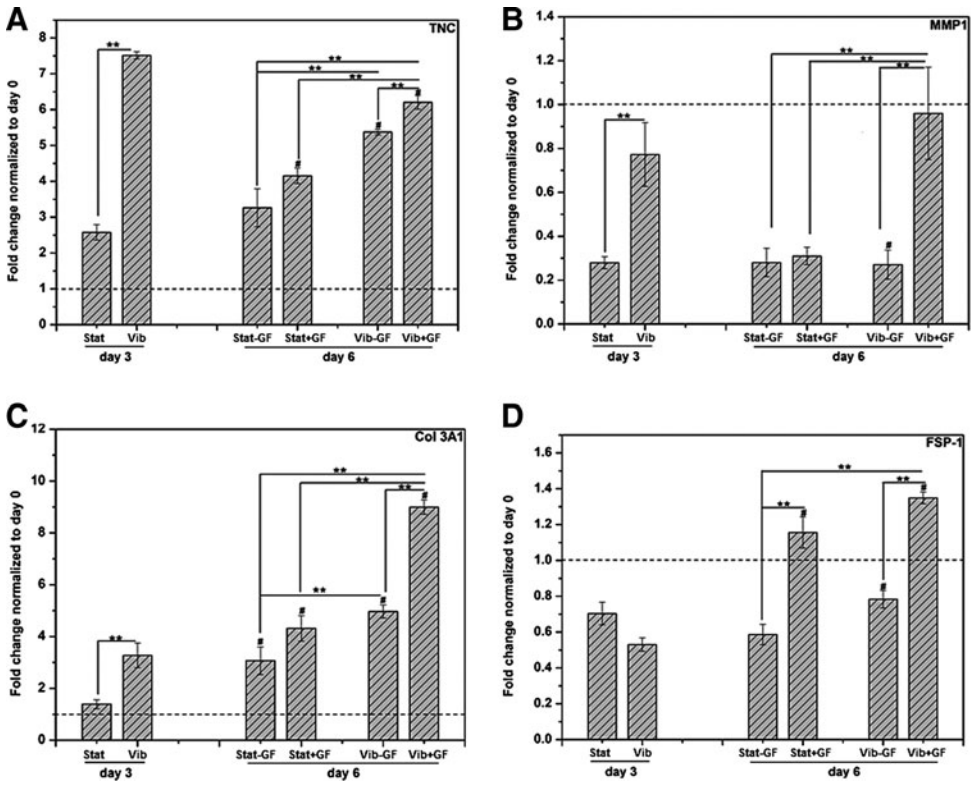

FIG. 4. Effects of the culture time and conditions on the expression of genes encoding fibroblastic hallmarks (**A**: tenascin-C (*TNC*), **B**: matrix metalloproteinase-1 (*MMP1*), **C**: *Col 3A1*, **D**: fibroblast-specific protein-1 (*FSP-1*)). The relative expression (fold change) was normalized to the level at day 0 (dashed baseline). #Significantly different compared with the corresponding static or dynamic culture at day 3 ($p<0.05$); **significantly different between the indicated groups ($p<0.05$).

compared with Vib at day 3. A similar trend was observed for Stat − GF and Stat + GF relative to Stat, however, the expression levels for Vib − GF and Vib + GF groups were higher than the Stat − GF and Stat + GF groups. No appreciable effect was introduced at day 6 by the CTGF treatment. The expression profile of *Col 1A1* (Fig. 3D) followed a distinct temporal pattern. Its relative expression steadily increased from day 0 to 6 for all the four groups, with the Vib + GF group exhibiting the highest level (2.71 ± 0.05) of *Col 1A1* expression. The 3-day vibratory culture moderately increased *Col 1A1* expression (1.67 ± 0.13 for Vib vs. 1.34 ± 0.10 for Stat). The regulatory effect of CTGF was more pronounced in groups with vibration history. The highest *Col 1A1* expression was observed when the vibratory preconditioning and CTGF treatment were both imposed (Vib + GF). Compared with the Stat − GF, *Col 1A1* expression by the Vib + GF group was $\sim$1.36 ($p<0.05$) fold higher.

Next, effects of mechanical and biochemical stimulations on the expression of genes encoding broad fibroblastic hallmarks were evaluated (Fig. 4).[18,26] Compared with the static culture, cells subjected to the 3-day, intermittent vibration exhibited a 3.01-fold increase (2.58 ± 0.22 for Stat vs. 7.52 ± 0.10 for Vib, $p<0.0001$) in *TNC* expression (Fig. 4A). Subsequent 3-day static culture significantly attenuated the *TNC* expression (Vib − GF and Vib + GF vs. Vib), independent of the media composition. With regard to the static groups, the Stat + GF group expressed a higher level of *TNC* than the Stat group ($p<0.05$). At day 6, the highest level of *TNC* expression was observed for the Vib + GF group, with a fold increase of $\sim$1.88 over the Stat − GF controls ($p<0.001$). The addition of CTGF to cultures with a vibration history (Vib + GF vs Vib − GF) also elicited a significant increase of *TNC* expression. The expression pattern for MMP1, a fibroblastic marker and a crucial ECM remodeling enzyme, is summarized in Figure 4B. During the initial 3 days of culture, the dynamically cultured MSCs (Vib, 0.77 ± 0.15) expressed *MMP1* at a level approximately 2.75 times higher ($p<0.05$) than the statically cultured counterparts (Stat, 0.28 ± 0.03). Compared with Stat − GF and Stat + GF groups, the Vib + GF group showed a marked upregulation ($\sim$3.43-fold, $p<0.05$) of *MMP1* expression at day 6. Contrary to TNC, prolonged culture reduced the MMP1 expression below the baseline level at day 0, although the combined vibration and CTGF treatment compensated the reduction.

Sequential vibration and CTGF treatments resulted in a synergistic enhancement in *Col 3A1* expression (Fig. 4C). Vibration alone increased *Col 3A1* level by $\sim$2.23-folds (Vib vs Stat, $p<0.01$). Addition of CTGF further increased *Col 3A1* expression. By day 6, the highest level of *Col 3A1* was detected in the Vib + GF group, $\sim$3.00 ($p<0.0001$) times higher than the Stat − GF group, $\sim$1.81 times higher ($p<0.05$) than the Vib − GF group, and $\sim$2.08-fold higher than the Stat + GF group ($p<0.01$). The expression pattern of *FSP-1* (Fig. 4D) was distinctly different from that for Col 3A1. The 3-day vibratory loading moderately attenuated the *FSP-1* expression. Compared with the Stat − GF group, CTGF-treatment triggered a $\sim$1.97-fold increase in *FSP-1* expression in the Stat + GF group. Similar enhancement was observed between Vib + GF and Vib − GF groups, albeit at a lower level ($\sim$1.72-fold, $p<0.05$). However, the fold change in *FSP-1* expression was found to be insignificant between Stat − GF and Vib − GF, and the Stat + GF and Vib + GF groups. Therefore, it is evident that CTGF is a more potent regulator of *FSP-1* expression than the high frequency vibration.

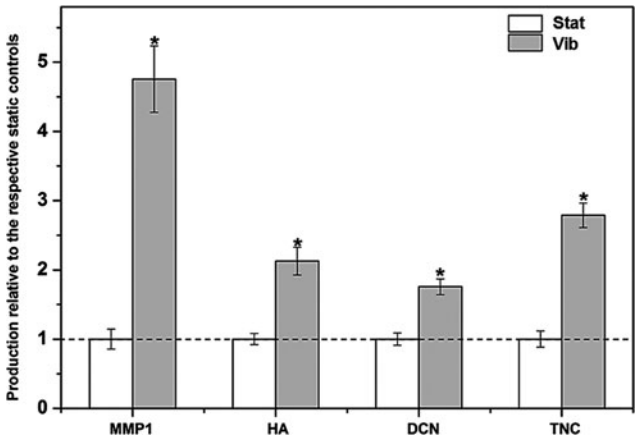

FIG. 5. Biochemical quantification of MMP1, HA, DCN, and TNC secreted by MSCs cultured on PCL scaffolds after the 3-day vibratory culture. The relative production of each component was normalized to the respective static controls (dashed baseline) at day 3. *Significantly different between the static and vibratory cultures ($p < 0.05$).

The chondrogenic, osteogenic, and adipogenic differentiation potentials of MSCs were analyzed by quantifying the mRNA levels of aggrecan (*ACAN*), alkaline phosphatase (*ALP*), and adipocyte Protein 2 (*aP2*) (Supplementary Fig. S2). Under the experimental conditions employed, cellular expression of *aP2* was not detectable by qPCR and the expression of *ACAN* was not statistically different among various groups at day 3 and 6. On the other hand, the combined treatment significantly attenuated *ALP* expression compared with either the Stat − GF aor the Stat + GF controls, and the *ALP* level expressed by the Vib + GF group at day 6 was close to the baseline level at day 0.

Finally, the effects of vibratory stimulations and CTGF treatment on protein synthesis were quantified by ELISA and western blotting. The ELISA results (Fig. 5) show that the high frequency vibration increased the cellular production of MMP1, HA, DCN, and TNC, relative to their static controls, with a fold increase of 4.81 ± 0.51 ($p < 0.005$), 2.12 ± 0.23 ($p < 0.01$), 1.85 ± 0.11 ($p < 0.0001$), and 2.82 ± 0.26 ($p < 0.0001$), respectively. The western blot analysis revealed that the augmentation in Col I synthesis was primarily governed by the CTGF treatment. Overall, the addition of CTGF to the cell culture media on day 3–6 resulted in > 2.5 ($p < 0.05$) fold increase in Col I synthesis, regardless of the culture conditions on day 0–3. In accordance with the qPCR results, the Vib + GF group produced the highest amount of Col III: over 16.0 times higher ($p < 0.001$) than the Stat − GF control group (Fig. 6C). Cells in the Vib − GF group also produced a larger amount of Col III than those in Stat − GF controls, but with a much lower fold difference (~4.1-fold). Thus, the ability of CTGF to enhance Col III synthesis depended on whether cells had

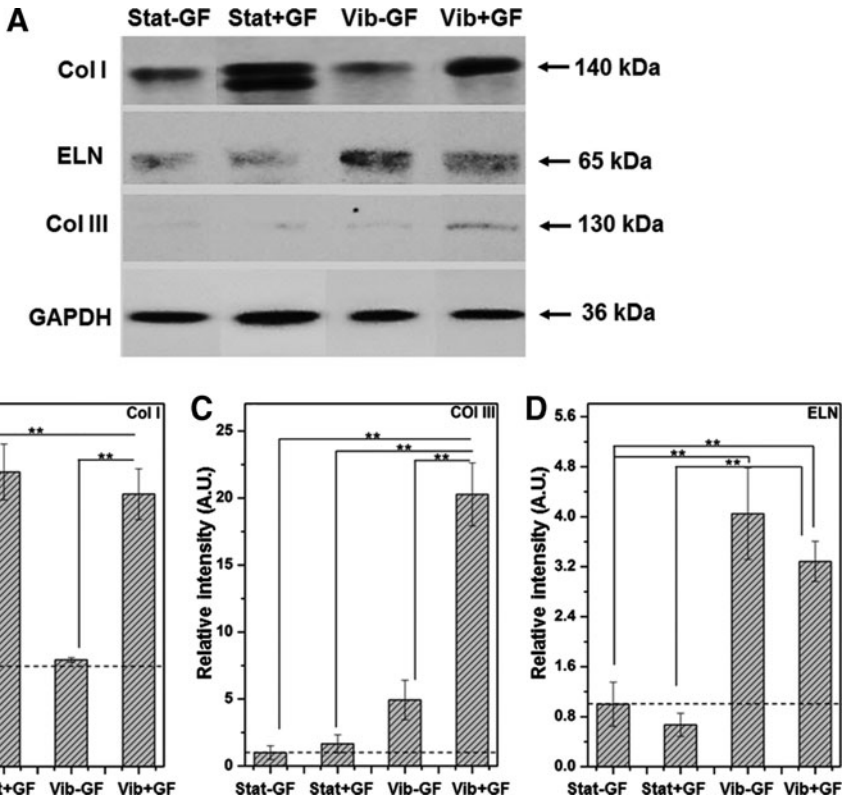

FIG. 6. **(A)** Western blot analysis of cellular synthesis of collagen I (Col I), collagen III (Col III), and elastin (ELN) after sequential vibration and CTGF treatments. Quantitative results **(B–D)** were obtained by densitometry analysis. The intensity of individual bands was normalized first to the corresponding GAPDH loading controls, then to the Stat − GF controls (dashed baseline). The presence of two Col I bands can be attributed to the presence of multiple post-translational isoforms (e.g., glycosylated or acylated adducts) or different building units being synthesized that were not resolved by electrophoresis [24]. Only the upper band corresponding to the 140 kDa product was analyzed. **Significantly different between the indicated groups ($p < 0.05$).

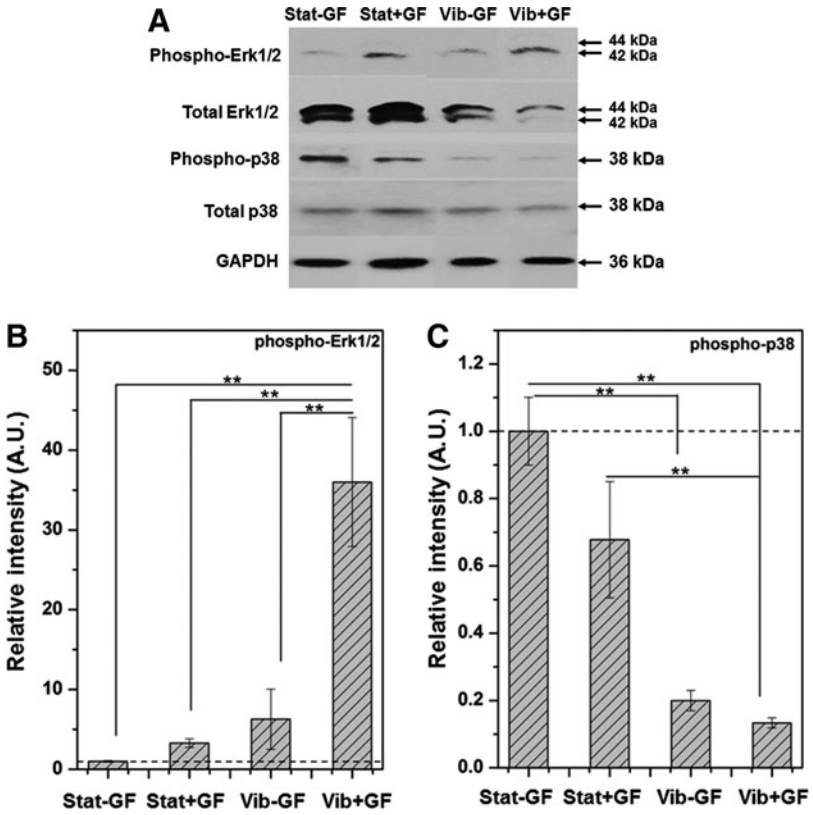

FIG. 7. Western blot analysis **(A)** of the activation of MAPK kinases: Erk1/2 and p38, after sequential vibration and CTGF treatments. The activation of Erk1/2 **(B)** or p38 **(C)** was analyzed by first normalizing the intensity of the phosphorylated (phospho-) Erk1/2 or p38 band to that of the total Erk1/2 or p38 respectively, then to the corresponding GAPDH loading controls. For comparison purposes, the results were further normalized against the Stat − GF controls (dashed baseline). **Significantly different between the indicated groups ($p < 0.05$).

experienced the dynamic vibration prior to the CTGF treatment. Quantification of ELN production by western blotting and by qPCR revealed a similar trend. Cells subjected to mechanical loading (Vib − GF and Vib + GF) produced > 3.0 more ELN than the respective controls (Stat − GF and Stat + GF, $p < 0.05$). CTGF treatment did not induce any appreciable changes in the synthesis of ELN, irrespective of the prior culture conditions.

Role of MAPK pathways in MSC's mechano- and biochemical sensing

The MAPK pathways can be activated by soluble biochemical factors or integrin-mediated cell-ECM interactions.[27,28] In the present study, we explored the potential of mechano- and biochemical stimulations on the activation of three MAP kinases: Erk1/2, c-Jun N-terminal kinase (JNK), and p38 (Fig. 7) at day 6. The phosphorylation of JNK was not detectable by western blotting under all conditions tested. Compared with the static controls (Stat − GF) cultured in the maintenance media, sequential vibration and CTGF treatment (Vib + GF) resulted in > 20-fold increase in Erk1/2 phosphorylation (Fig. 7B, $p < 0.001$). CTGF had a more profound effect on Erk/12 activation in cells with vibration history than in those cultured statically prior to the growth factor treatment; the level of phosphorylated Erk1/2 in the Vib + GF group was ~7.1 times higher than in the Vib − GF group, whereas the difference between the Stat + GF and the Stat − GF was only 3.9-folds. Interestingly, stimulation of MSCs with combined vibration and CTGF treatment significantly suppressed p38 phosphorylation and the vibratory loading was the major contributing factor. A close to 5.0-fold reduction was observed when cells were subjected to the 3-day vibratory culture irrespective of the media composition in the subsequent 3-day static culture (Stat − GF/Vib − GF = 5; Stat + GF/Vib + GF = 5).

To further ascertain the involvement of Erk1/2 pathways in cellular mechano- and chemical sensing, Erk1/2 was inactivated using U0126, a well-known inhibitor of Erk1/2 upstream mediator (MEK1/2). The Picogreen DNA assay did not reveal any significant alteration of cell viability in the Erk1/2 inhibition study (data not shown), suggesting the specific inhibition regime employed was cytocompatible. At the mRNA level, the U0126 treatment attenuated the cellular expression of *DCN* (Fig. 8A), *Col 3A1* (Fig. 8B), *TNC* (Fig. 8C), and *MMP1* (Fig. 8D). The addition of U0126 did not significantly alter the gene expression profiles for *DCN*, *Col3A1*, and *MMP1* among the four experimental groups under each setting (+/− U0126), suggesting other signaling pathways may be also implicated in the current mechanical/biochemical sensing. For instance, the highest expression level of *DCN* was detected from the Vib + GF group in the absence of U0126. With the addition of U0126, the Vib + GF group still expressed the highest level of *DCN* among all four groups tested, but the level was close to that of the baseline controls (Stat − GF-U0126).

Blocking the Erk1/2 pathway diminished MSC's sensitivity toward the combined vibration and CTGF treatment in terms of the *Col 3A1* expression (Fig. 9B). Similarly, the U0126 treatment decreased the *TNC* expression in Stat + GF and Vib − GF groups compared with their respective controls without U0126 (Fig. 9C). Although the U0126 treatment resulted in a 4.6-fold reduction in *MMP1* expression by the Vib + GF group relative to the U0126-free controls

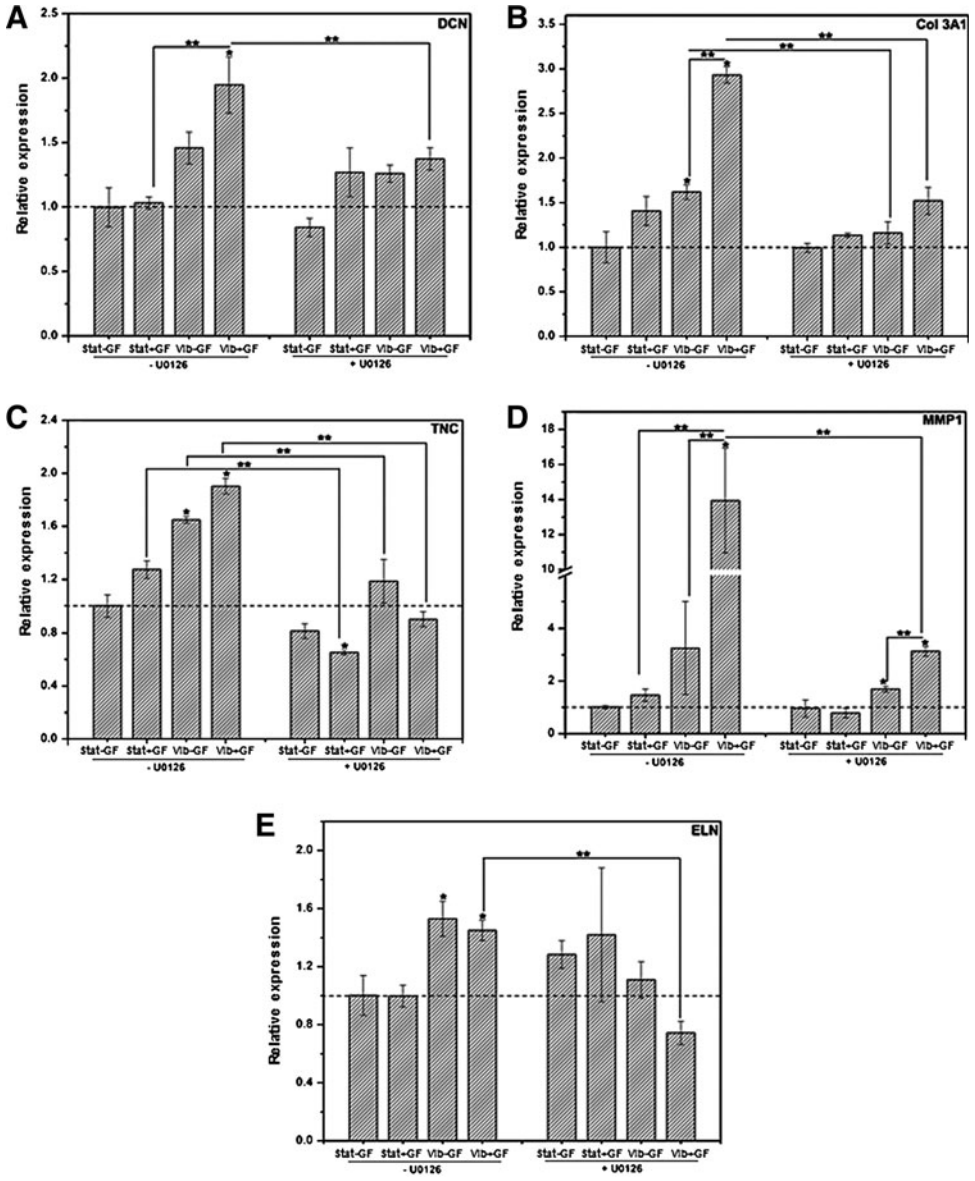

FIG. 8. Effects of the Erk1/2 inhibition by U0126 on MSC gene expression after sequential vibration and CTGF treatments (**A**: *DCN*, **B**: *Col 3A1*, **C**: *TNC*, **D**: *MMP1*, **E**: *ELN*). Gene expression was evaluated by *q*PCR and the relative expression level was normalized to the respective Stat − GF controls without U0126 (dashed baseline). *Significantly different compared with the Stat − GF control groups without U0126 treatment ($p < 0.05$); **significantly different between the indicated groups ($p < 0.05$).

($p < 0.05$, Fig. 8D), the expression level was still higher ($\sim$3.2-fold, $p < 0.001$) than that of the Stat − GF group without U0126. Thus, the upregulation of *MMP1* expression may only be partially controlled by Erk1/2. The vibration-induced upregulation of *ELN* expression was abolished by blocking Erk1/2 (Fig. 8E). The U0126 treatment did not cause a significant alteration of *ELN* expression for the Stat − GF and Stat + GF groups, but reduced the expression in the Vib + GF and Vib − GF groups near the baseline level ($p < 0.05$ for the Vib + GF group). With regard to the Vib + GF groups, the addition of U0126 resulted in a reduction of the expression of *DCN*, *Col 3A1*, *TNC*, and *MMP1* by 1.4, 1.9, 2.1, and 4.5-folds (all $p < 0.05$), respectively. Moreover, the U0126 treatment effectively reduced the expression of *DCN*, *Col 3A1*, and *TNC* to close to the baseline levels. These results indicate that the combinatory effects from vibration and CTGF on gene expression were completely abolished by inhibiting the Erk1/2 pathway.

At the protein level, vibration and CTGF cooperatively promoted the cellular production of DCN; the Vib + GF group produced 2.4 ± 0.4 times more (Fig. 9A, $p < 0.05$) DCN than the Stat − GF control, corroborating the qPCR results discussed earlier. This stimulatory effect was significantly compromised by the U0126 treatment. In the Vib − GF and Vib + GF groups, U0126 treatment decreased the DCN production by approximately two folds ($p < 0.05$) relative to the respective no U0126 controls. In the U0126-treated groups, a fold difference of 1.6 ± 0.1 and 2.2 ± 0.1 was found between the Stat + GF/Stat − GF and Vib + GF/Vib − GF groups, respectively, implying the CTGF-induced DCN synthesis was not completely regulated by Erk1/2.

In the absence of U0126, the MMP1 secretion was elevated (2.2 ± 0.2-fold, $p < 0.01$) in the Vib + GF group compared with the Stat − GF group, consistent with the qPCR results described earlier. Erk1/2 inhibition did not result in a profound alteration in MMP1 secretion (Fig. 9B) for all four experimental groups. The TNC production at the protein level (Fig. 9C) under U0126-free culture also agrees with its qPCR results. The dynamic vibration had a profound effect on the TNC production; compared with the Stat − GF group,

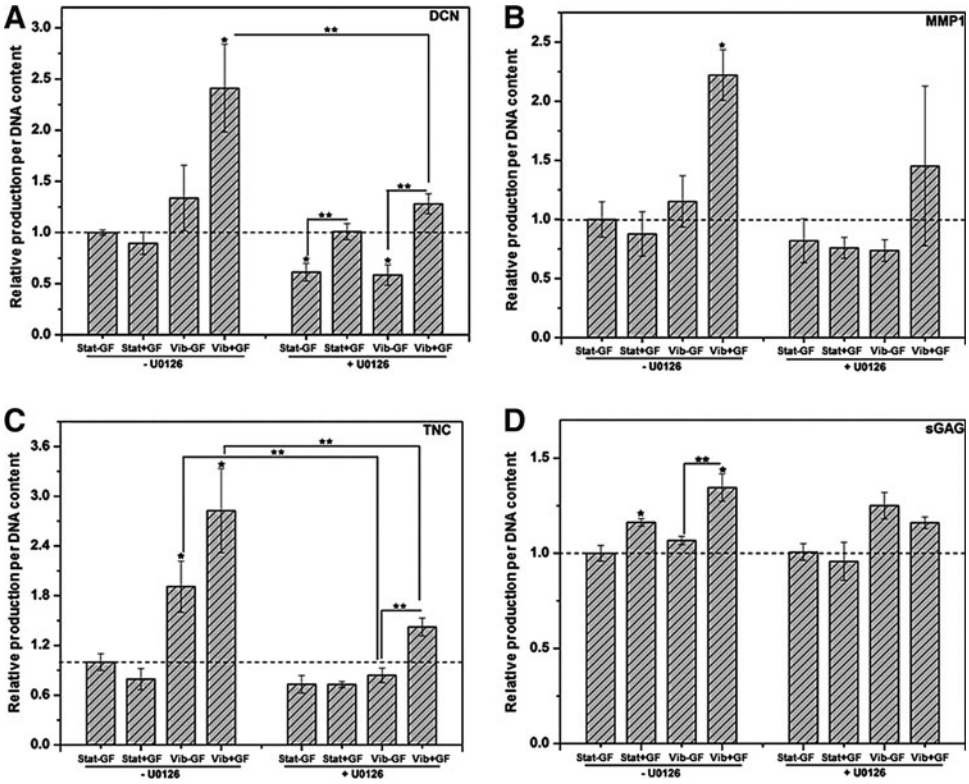

FIG. 9. Effects of the Erk1/2 inhibition by U0126 on ECM synthesis after sequential vibration and CTGF treatments (**A**: *DCN*, **B**: *MMP1*, **C**: *TNC*, **D**: *sGAG*). The relative production of each ECM component (per DNA content) was normalized to their respective Stat − GF group without U0126 control groups (dashed baseline). *Significantly different compared with the Stat − GF control groups without U0126 treatment ($p < 0.05$); **significantly different between the indicated groups ($p < 0.05$).

Vib − GF and Vib + GF groups produced 1.9 ± 0.3 and 2.8 ± 0.5 times more TNC. The addition of U0126 led to an overall reduction of TNC secretion. Upon U0126 treatment, the TNC production by the Vib − GF and Vib + GF groups was reduced ($p < 0.05$) near the level of the Stat − GF controls, although the Vib + GF group (1.4 ± 0.1) was still higher ($p < 0.05$) than the Vib − GF group (0.8 ± 0.1). In the absence of U0126, the Vib + GF group produced the highest amount of sGAG (1.35 ± 0.07-fold relative to the Stat − GF control, Fig. 9D). Compared to the Stat − GF controls, the Stat + GF group produced $\sim 17\%$ more ($p < 0.05$) sGAG, and this increment was abolished by U0126. A similar trend was observed between the Vib − GF and Vib + GF groups, suggesting the CTGF-induced sGAG synthesis was regulated by Erk1/2.

Discussion

The goal of this investigation is to identify *in vitro* culture conditions that provide vocal fold-like environment to modulate MSC behaviors and to guide them toward a vocal fold fibroblastic phenotype. We demonstrated that vibratory stimulations and CTGF, when sequentially introduced to MSCs cultured on fibrous PCL scaffolds, effectively modulated cellular functions in terms of ECM synthesis and remodeling. Physiologically relevant mechanical forces have been shown to be potent regulators of tissue-specific stem cell differentiation and matrix remodeling.[19–21,29] We have previously reported a vocal fold bioreactor capable of delivering vibratory stimulations to the cultured cells at phonation frequencies.[6,30] We found that MSCs attached to fibrous PCL scaffolds and exposed to high frequency vibrations were more actively engaged in the synthesis and remodeling of vocal fold-relevant ECM proteins.[6] A similar 1 h-on-1 h-off regime with a net total of 6 h daily vibration was employed in the current study, but at a shorter duration (3 days vs. 7 days).[6,31] In the context of vocal folds, DCN, MMP1, and HA are generally classified as ''anti-scarring'' or ''lubricant'' molecules.[6] The enhanced expression of these components, both at the mRNA or protein levels, in response to the 3-day vibrations, suggests that MSCs may have adapted to the vibrational loading by rapidly reorganizing and remodeling their matrix components for efficient stress dissipation.[6,32] Overall, the 3-day vibratory loading had a profound effect on MSCs' ability to synthesize vocal fold-relevant ECM components. The newly synthesized ECMs, in turn, may offer a feedback mechanism to modulate the original stem cell niche, potentially rendering MSCs to respond to the subsequent CTGF treatment more effectively.[33]

When the dynamic loading was immediately followed by a 3-day static culture in the presence of CTGF, cellular production of fibrous matrix proteins, interstitial amorphous components, and ECM-remodeling enzymes, was simultaneously regulated. Elastin and collagen I, the major fibrous proteins rich in the intermediate and deep layers of vocal fold lamina propria, primarily provides the tissue with strength, extensibility, and elasticity that are crucial for voice production.[3,34] The elastin expression was predominantly regulated by mechanical cues, and this stimulatory effect was not abolished even after an additional 3-day static rest (with or without CTGF). On the other hand, the mRNA level of *Col 1A1* was cooperatively enhanced by the combined vibration and CTGF treatment (Fig. 3D). When applied alone, vibration or CTGF did not have a profound stimulatory effect on *Col 1A1* expression, even for longer

time (>6 days).[6,15] Interestingly, at the protein level, Col I production was predominantly controlled by CTGF (Fig. 6B) and the stimulatory effects of vibration was not manifested at the protein level. Such a discrepancy can be attributed to the complex translational and post-translational events occurring during collagen biosynthesis, in which the biochemical factors (CTGF) may play a more defining role than the mechanical signals.[35]

Tissue homeostasis relies on the balance between matrix synthesis and degradation.[36] The secretion of MMP1 is known to be sensitive to mechanical stresses and is highly time-dependent.[6,37] Our stimulation strategy not only cooperatively fostered the accumulation of major fibrous ECM proteins but also concomitantly elevated the MMP1 secretion. The 3-day vibratory preconditioning significantly increased MMP1 production, and this elevated level was maintain through day 6 only when CTGF was subsequently introduced. These findings imply that the combined vibration and growth factor effectively maintained MSCs in an activated state to achieve a balanced ECM remodeling.[37] Collectively, these results confirm the ability of vibration stresses and the soluble factors to alter the mechanical properties of the vocal fold tissues.[38–40]

In addition to fibrous proteins, amorphous ECM components, such as Col III, GAGs and proteoglycans are also indispensable for the proper function of vocal folds. Col III forms reticular fibers to provide the extensibility of load-bearing tissues and plays a crucial role in Col I fibrillogenesis. Our results show that the mechanical and biochemical stimulations synergistically enhanced Col III synthesis, both at the mRNA (Fig. 4C) and the protein levels (Fig. 6C). In fact, the conducive effect of CTGF was amplified when the cells were dynamically pretreated. The assembly and organization of collagen fibers are also intimately mediated by a small proteoglycan, DCN. In the current study, significantly increased DCN production (Figs. 3B and 9A) was attained only when the vibratory preconditioning and CTGF treatment were combined. Overall, MSCs cultured on PCL scaffolds and subjected to the sequential mechanical and biochemical stimulations are actively engaged in the early phase of matrix assembly, organization, and remodeling.[41]

Enriched in the ILP of the vocal fold, HA not only contributes to the maintenance of tissue viscoelasticity but also plays an important role in the wound healing of tissue.[42,43] The 3-day vibratory stimulation resulted in an increase in HA production. However, by day 6, the modulatory effects were abolished irrespective of the culture history or the media composition (data not shown). These findings indicate that the production of HA was transient and the dual stimuli applied herein may be counteracting with each other on HA biosynthesis. Contrarily, the CTGF treatment has elicited a positive effect on sGAG production (irrespective of the dynamic loading). CTGF enhanced sGAG production predominantly with the vibratory preconditioning offering an additional effect (Fig. 9D). This additive effect may be attributed to the ability of neo-synthesized sGAGs to sequester CTGF, thereby potentiating its biological activities.[17,44]

The presence of TNC in adult vocal fold LP has not been confirmed yet. Because TNC is primarily confined to tissues experiencing high tensile stresses,[32,44] it is not unreasonable to speculate its involvement in the early development of vocal fold tissues. We found that CTGF cooperated with the vibratory stimulations to promote the TNC expression at both the mRNA and the protein levels (Figs. 4A and 9C). Indeed, high frequency vibrations and CTGF, separately, has already been found to be potent regulators of TNC expression.[6,18] The cooperativity of mechanical and biochemical signals underlines the importance of creating tissue-like microenvironment to foster neo-tissue formation.

To gain a mechanistic understanding of our results, the involvement of MAPK pathways in cellular mechano- and biochemical sensing was explored. Various subsets of MAPKs, such as Erk1/2, stress-activated protein kinase p38, and JNK can be activated by mechanical strains and mitogenic stimuli.[44,45] Our results show that vibration followed by CTGF gave rise to the highest level of Erk1/2 activation and that cells with vibratory history were more susceptible to CTGF stimulation. The phosphorylation of p38, however, followed an opposite trend. The combined treatment resulted in a significant deactivation of p38. We speculate that p38 and Erk1/2 might be able to negatively impact each other. The interference among different MAPK family members has been demonstrated in several previous reports.[46,47] Overall, the dynamic balance between Erk1/2 and p38 may be crucial in determining cell fate.[48]

To further ascertain the involvement of Erk1/2 pathways in the mechanical-biochemical sensing, parallel experiments were carried in the presence of U0126, a chemical inhibitor of Erk1/2. The upregulation of *DCN*, *Col 3A1*, *TNC*, *MMP1*, and *ELN* (at the mRNA level) by the combined vibration and CTGF treatment was diminished by U0126. A similar inhibitory effect was observed for DCN, TNC, and MMP1 at protein levels, albeit to a lesser extent. These results suggest that the Erk1/2 pathways were more involved in the early transcriptional stages of ECM biosynthesis than the later ones that require multiple steps of posttranslational modifications. Our results show that, compared to the mechanical stress, CTGF plays a more dominant role in promoting cellular production of sGAG and that the CTGF-induced enhancement was completely countered by blocking the Erk1/2 activity. Therefore, the sGAG production was primarily regulated by CTGF through Erk1/2 MAPK pathway, in agreement with previous reports.[49]

The vibratory loading may regulate ECM synthesis directly by evoking intracellular signaling pathways that regulate the genes, or indirectly by triggering the release of paracrine factors,[50] and integrin engagement in these processes has been well established.[51] On the other hand, CTGF is well known to regulate cell adhesion, migration, and DNA and ECM synthesis via the interaction with a variety of receptors, extracellular ligands, and various co-factors (e.g., TGF-β, EGF).[17,52,53] When CTGF was introduced after the vibration, interactions between CTGF receptors and integrins may contribute to the observed cooperative effects from mechanical and biochemical signals.[54] In response to the vibrational stresses, integrin receptors may become clustered and be reinforced.[6] Integrin-regulated clustering of various receptor kinases, together with their downstream targets, may have amplified the signaling of CTGF to MAPK or other pathways involved in cell proliferation, differentiation, and ECM remodeling.[32]

We have previously demonstrated the efficacy of physiologically relevant high frequency vibrations and CTGF

alone on the fibroblastic commitment of MSCs.[6,15] Here, we show that these mechanical and biochemical cues, when introduced sequentially, are more conducive to MSC's adaptation of VFF-like behaviors. Vibratory preconditioning essentially primed MSCs to an activated state that more effectively respond to the subsequent biochemical cues. Under the conditions employed in our study, classical MSC tri-lineage differentiation pathways (chondro-, osteo-, and adipogenesis) was suppressed, or at least not evoked. The enhanced production of broad fibroblastic hallmarks: Col I, Col III, *FSP-1*, TNC, and MMP1 further corroborate the notion of the fibroblastic commitment. Future efforts are needed to identify the matrix or cellular markers that are more specific for human vocal fold tissues.

Conclusion

To emulate the microenvironment of developing vocal folds, physiologically relevant high frequency vibrations and CTGF were sequentially introduced MSCs cultured on fibrous PCL scaffolds. Cells were dynamically cultured with a 1-h-on-1-h-off vibration at 200 Hz for 3 days, followed by a 3-day static culture in the presence of soluble CTGF. The vibratory stimulations and the soluble growth factors cooperatively mediated MSCs behaviors, leading to an accelerated ECM synthesis and a balanced ECM remodeling. Importantly, the vibratory stresses rendered MSCs more responsive to the subsequent CTGF treatment. Our mechanistic studies show that Erk1/2 pathways are involved in cellular responses to mechano- and biochemical signals. The 6-day combined vibration and CTGF treatment effectively induced the fibroblastic commitment of MSCs. Our study points to the complexity of mechanical and biochemical signaling and underscores the importance of rational combination of distinct stimuli to regulate MSC behaviors for vocal fold tissue engineering.

Acknowledgments

We thank the Keck Electron Microscopy Lab and Dr. Chaoying Ni and Mr. Chang Liu for SEM assistance. This work is funded by the National Institutes of Health (NIDCD, R01008965 and R01DC011377). ABZ acknowledges NSF Integrative Graduate Education and Research Traineeship (IGERT) program for funding.

Disclosure Statement

No competing financial interests exist.

References

1. Titze, I.R. On the relation between subglottal pressure and fundamental-frequency in phonation. J Acoust Soc Am **85,** 901, 1989.
2. Howard, D.M. Raising public awareness of acoustic principles using voice and speech production. J Acoust Soc Am **131,** 2405, 2012.
3. Hansen, J.K., and Thibeault, S.L. Current understanding and review of the literature: vocal fold scarring. J Voice **20,** 110, 2006.
4. Hirano, S. Current treatment of vocal fold scarring. Curr Opin Otolaryngol Head Neck Surg **13,** 143, 2005.
5. Kutty, J.K., and Webb, K. Tissue engineering therapies for the vocal fold lamina propria. Tissue Eng Part B Rev **15,** 249, 2009.
6. Tong, Z., Duncan, R.L., and Jia, X. Modulating the behaviors of mesenchymal stem cells via the combination of high frequency vibratory stimulations and fibrous scaffolds. Tissue Eng Part A **19,** 1862, 2013.
7. Pittenger, M.F., Mackay, A.M., Beck, S.C., Jaiswal, R.K., Douglas, R., Mosca, J.D., *et al.* Multilineage potential of adult human mesenchymal stem cells. Science **284,** 143, 1999.
8. Hanson, S.E., Kim, J., Johnson, B.H.Q., Bradley, B., Breunig, M.J., Hematti, P., *et al.* Characterization of mesenchymal stem cells from human vocal fold fibroblasts. Laryngoscope **120,** 546, 2010.
9. Hwang, N.S., Varghese, S., and Elisseeff, J. Controlled differentiation of stem cells. Adv Drug Deliv Rev **60,** 199, 2008.
10. Metallo, C.M., Mohr, J.C., Detzel, C.J., de Pablo, J.J., Van Wie, B.J., and Palecek, S.P. Engineering the stem cell microenvironment. Biotechnol Prog **23,** 18, 2007.
11. Fisher, M.B., and Mauck, R.L. Tissue engineering and regenerative medicine: recent innovations and the transition to translation. Tissue Eng Part B Rev **19,** 1, 2013.
12. Newman, S.R., Butler, J., Hammond, E.H., and Gray, S.D. Preliminary report on hormone receptors in the human vocal fold. J Voice **14,** 72, 2000.
13. Sato, K., and Hirano, M. Histologic investigation of the macula flava of the human newborn vocal fold. Ann Otol Rhinol Laryngol **104,** 556, 1995.
14. Sato, K., Hirano, M., and Nakashima, T. Fine structure of the human newborn and infant vocal fold mucosae. Ann Otol Rhinol Laryngol **110,** 417, 2001.
15. Tong, Z., Sant, S., Khademhosseini, A., and Jia, X. Controlling the fibroblastic differentiation of mesenchymal stem cells via the combination of fibrous scaffolds and connective tissue growth factor. Tissue Eng Part A **17,** 2773, 2011.
16. Gad, Y.Z., Berkovitz, G.D., Migeon, C.J., and Brown, T.R. Studies of up-regulation of androgen receptors in genital kkin fibroblasts. Mol Cell Endocrinol **57,** 205, 1988.
17. Chen, C.C., and Lau, L.F. Functions and mechanisms of action of CCN matricellular proteins. Int J Biochem Cell Biol **41,** 771, 2009.
18. Lee, C.H., Shah, B., Moioli, E.K., and Mao, J.J. CTGF directs fibroblast differentiation from human mesenchymal stem/stromal cells and defines connective tissue healing in a rodent injury model. J Clin Invest **120,** 3340, 2010.
19. Kim, B.S., Nikolovski, J., Bonadio, J., and Mooney, D.J. Cyclic mechanical strain regulates the development of engineered smooth muscle tissue. Nat Biotechnol **17,** 979, 1999.
20. Kim, Y.J., Sah, R.L.Y., Grodzinsky, A.J., Plaas, A.H.K., and Sandy, J.D. Mechanical regulation of cartilage biosynthetic behavior—physical stimuli. Arch Biochem Biophys **311,** 1, 1994.
21. Wang, J.H.C., and Thampatty, B.P. Mechanobiology of adult and stem cells. Int Rev Cell Mol Biol **271,** 301, 2008.
22. Hartman, O., Zhang, C., Adams, E.L., Farach-Carson, M.C., Petrelli, N.J., Chase, B.D., *et al.* Biofunctionalization of electrospun PCL-based scaffolds with perlecan domain IV peptide to create a 3-D pharmacokinetic cancer model. Biomaterials **31,** 5700, 2010.
23. Ryseck, R.P., Macdonaldbravo, H., Mattei, M.G., and Bravo, R. Structure, mapping, and expression of fisp-12, a

growth factor-inducible gene encoding a secreted cysteine-rich protein. Cell Growth Differ **2,** 225, 1991.
24. Hoemann, C.D. Molecular and biochemical assays of cartilage components. Methods Mol Med **101,** 127, 2004.
25. Megelski, S., Stephens, J.S., Chase, D.B., and Rabolt, J.F. Micro- and nanostructured surface morphology on electrospun polymer fibers. Macromolecules **35,** 8456, 2002.
26. Doroski, D.M., Levenston, M.E., and Temenoff, J.S. Cyclic tensile culture promotes fibroblastic differentiation of marrow stromal cells encapsulated in poly(ethylene glycol)-based hydrogels. Tissue Eng Part A **16,** 3457, 2010.
27. Robinson, M.J., and Cobb, M.H. Mitogen-activated protein kinase pathways. Curr Opin Cell Biol **9,** 180, 1997.
28. Morino, N., Mimura, T., Hamasaki, K., Tobe, K., Ueki, K., Kikuchi, K., *et al.* Matrix/integrin interaction activates the mitogen-activated protein kinase, p44erk-1 and p42erk-2. J Biol Chem **270,** 269, 1995.
29. Guilak, F., Cohen, D.M., Estes, B.T., Gimble, J.M., Liedtke, W., and Chen, C.S. Control of stem cell fate by physical interactions with the extracellular matrix. Cell Stem Cell **5,** 17, 2009.
30. Farran, A.J.E., Teller, S.S., Jia, F., Clifton, R.J., Duncan, R.L., and Jia, X. Design and characterization of a dynamic vibrational culture system. J Tissue Eng Reg Med **7,** 213, 2013.
31. Masuda, T., Ikeda, Y., Manako, H., and Komiyama, S. Analysis of vocal abuse—fluctuations in phonation time and intensity in 4 groups of speakers. Acta Oto-Laryngol **113,** 547, 1993.
32. Chiquet, M., Gelman, L., Lutz, R., and Maier, S. From mechanotransduction to extracellular matrix gene expression in fibroblasts. Biochim Biophys Acta **1793,** 911, 2009.
33. Peerani, R., and Zandstra, P.W. Enabling stem cell therapies through synthetic stem cell-niche engineering. J Clin Invest **120,** 60, 2010.
34. Moore, J., and Thibeault, S. Insights into the role of elastin in vocal fold health and disease. J Voice **26,** 269, 2012.
35. Fessler, J.H., Doege, K.J., Duncan, K.G., and Fessler, L.I. Biosynthesis of collagen. J Cell Biochem **28,** 31, 1985.
36. Cox, T.R., and Erler, J.T. Remodeling and homeostasis of the extracellular matrix: implications for fibrotic diseases and cancer. Dis Models Mech **4,** 165, 2011.
37. Jean, C., Gravelle, P., Fournie, J.J., and Laurent, G. Influence of stress on extracellular matrix and integrin biology. Oncogene **30,** 2697, 2011.
38. Gunter, H.E. Modeling mechanical stresses as a factor in the etiology of benign vocal fold lesions. J Biomech **37,** 1119, 2004.
39. Titze, I.R. Mechanical stress in phonation. J Voice **8,** 99, 1994.
40. Titze, I.R., Hitchcock, R.W., Broadhead, K., Webb, K., Li, W., Gray, S.D., *et al.* Design and validation of a bioreactor for engineering vocal fold tissues under combined tensile and vibrational stresses. J Biomech **37,** 1521, 2004.
41. Carver, W., Nagpal, M.L., Nachtigal, M., Borg, T.K., and Terracio, L. Collagen expression in mechanically stimulated cardiac fibroblasts. Circ Res **69,** 116, 1991.
42. Branski, R.C., Verdolini, K., Sandulache, V., Rosen, C.A., and Hebda, P.A. Vocal fold wound healing: a review for clinicians. J Voice **20,** 432, 2006.
43. Hammond, T.H., Zhou, R.X., Hammond, E.H., Pawlak, A., and Gray, S.D. The intermediate layer: A morphologic study of the elastin and hyaluronic acid constituents of normal human vocal folds. J Voice **11,** 59, 1997.
44. Kjaer, M. Role of extracellular matrix in adaptation of tendon and skeletal muscle to mechanical loading. Physiol Rev **84,** 649, 2004.
45. Roux, P.P., and Blenis, J. ERK and p38 MAPK-activated protein kinases: a family of protein kinases with diverse biological functions. Microbiol Mol Biol Rev **68,** 320, 2004.
46. Hoefen, R.J., and Berk, B.C. The role of MAP kinases in endothelial activation. Vasc Pharmacol **38,** 271, 2002.
47. Cheng, B., Song, J., Zou, Y., Wang, Q., Lei, Y.S., Zhu, C.L., *et al.* Responses of vascular smooth muscle cells to estrogen are dependent on balance between ERK and p38 MAPK pathway activities. Int J Cardiol **134,** 356, 2009.
48. Xia, Z.G., Dickens, M., Raingeaud, J., Davis, R.J., and Greenberg, M.E. Opposing effects of Erk and Jnk-P38 Map kinases on apoptosis. Science **270,** 1326, 1995.
49. Gao, X.X., Li, J.Z., Huang, H.C., and Li, X.M. Connective tissue growth factor stimulates renal cortical myofibroblast-like cell proliferation and matrix protein production. Wound Repair Regen **16,** 408, 2008.
50. Chiquet, M., Reneda, A.S., Huber, F., and Fluck, M. How do fibroblasts translate mechanical signals into changes in extracellular matrix production? Matrix Biol **22,** 73, 2003.
51. Shyy, J.Y.J., and Chien, S. Role of integrins in cellular responses to mechanical stress and adhesion. Curr Opin Cell Biol **9,** 707, 1997.
52. Grotendorst, G.R., and Duncan, M.R. Individual domains of connective tissue growth factor regulate fibroblast proliferation and myofibroblast differentiation. Faseb J **19,** 729, 2005.
53. Shi-Wen, X., Leask, A., and Abraham, D. Regulation and function of connective tissue growth factor/CCN2 in tissue repair, scarring and fibrosis. Cytokine Growth Factor Rev **19,** 133, 2008.
54. Ross, R.S. Molecular and mechanical synergy: cross-talk between integrins and growth factor receptors. Cardiovasc Res **63,** 381, 2004.

Address correspondence to:
Xinqiao Jia, PhD
Department of Materials Science and Engineering
University of Delaware
201 DuPont Hall
Newark, DE 19716

E-mail: xjia@udel.edu

Received: August 14, 2013
Accepted: January 22, 2014
Online Publication Date: February 27, 2014